Addition of blood to a phycogenic bone substitute leads to increased *in vivo* vascularization

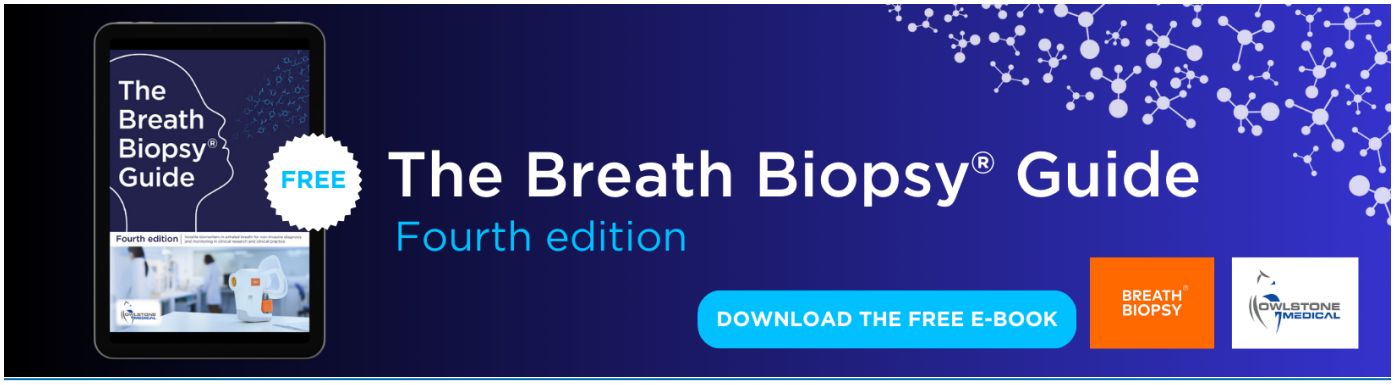

Biomedical Materials

PAPER

Addition of blood to a phycogenic bone substitute leads to increased *in vivo* vascularization

Mike Barbeck[1,2,7], Stevo Najman[3,7], Sanja Stojanović[3], Žarko Mitić[4], Jelena M Živković[3], Joseph Choukroun[5], Predrag Kovačević[5], Robert Sader[1], C James Kirkpatrick[2] and Shahram Ghanaati[1,2]

[1] Frankfurt Orofacial Regenerative Medicine (FORM) Lab, Department for Oral, Cranio-Maxillofacial and Facial Plastic Surgery, Medical Center of the Goethe University, Theodor-Stern-Kai 7, D-60590, Frankfurt, Germany
[2] Repair-Lab, Institute of Pathology, University Medical Center of the Johannes Gutenberg University, Mainz, Germany
[3] University of Niš, Faculty of Medicine, Department for Cell and Tissue Engineering, Institute of Biology and Human Genetics, Niš, Serbia
[4] University of Niš, Faculty of Medicine, Department of Pharmacy, Niš, Serbia
[5] Private practice, Pain Therapy Center, Nice, France
[6] University of Niš, Faculty of Medicine, Clinic of Plastic and Reconstructive Surgery, Niš, Serbia

E-mail: shahram.ghanaati@kgu.de

Keywords: Algipore®, blood addition, multinucleated giant cells, bone substitute, vascularization

OPEN ACCESS

RECEIVED
16 February 2015

REVISED
10 August 2015

ACCEPTED FOR PUBLICATION
17 August 2015

PUBLISHED
11 September 2015

Abstract

The present study aimed to analyze the effects of the addition of blood to the phycogenic bone substitute Algipore® on the severity of *in vivo* tissue reaction. Initially, Fourier-transform infrared spectroscopy (FTIR) of the bone substitute was conducted to analyze its chemical composition. The subcutaneous implantation model in Balb/c mice was then applied for up to 30 d to analyze the tissue reactions on the basis of specialized histochemical, immunohistochemical, and histomorphometrical methods.

The data of the FTIR analysis showed that the phycogenic bone substitute material is mainly composed of hydroxyapatite with some carbonate content. The *in vivo* analyses revealed that the addition of blood to Algipore® had a major impact on both angiogenesis and vessel maturation. The higher vascularization seemed to be based on significantly higher numbers of multinucleated TRAP-positive cells. However, mostly macrophages and a relatively low number of multinucleated giant cells were involved in the tissue reaction to Algipore®.

The presented data show that the addition of blood to a bone substitute impacts the tissue reaction to it. In particular, the immune response and the vascularization were influenced, and these are believed to have a major impact on the regenerative potential of the process of bone tissue regeneration.

1. Introduction

The regeneration of bone defects and bone formation prior to implant insertion for augmentation in the maxilla often require the application of bone substitute materials. In recent decades, many different bone substitutes have been tested that should replace the need for autologous bone transplants, whose application is accompanied by manifold side effects due to the harvesting surgical procedure [1, 2]. In addition to alternatives such as allogeneic and xenogeneic materials, which have been critically scrutinized based on reports about the inadequacy of their purification methods and ethical aspects, many types of synthetic bone substitute materials based on calcium phosphates with different chemical and physical characteristics have been tested for their application in bone tissue regeneration [3–6]. However, little knowledge exists about what physicochemical characteristics a synthetic bone substitute has to provide for an optimal level of bone regeneration. Thus, other naturally derived bone substitute materials based on hydroxyapatite such as from corals that possess physicochemical characteristics favorable for bone tissue repair have been developed to overcome the issues of the previously mentioned material classes [7]. Also, the calcium-based crust of the marine algae *Corallina officinalis* has been shown to be applicable as bone substitute after its thermal

[7] These authors contributed equally.

conversion to hydroxyapatite and its purification from organic components [8]. Thereby, the final material has a unique interconnecting tubular structure with a microporosity of 5–10 μm [8]. The bone substitute Algipore® is the sole representative of the group of algae-derived or so-called phycogenic materials. In recent decades, many different studies describe its successful clinical functionality for bone repair as well as the tissue reactions to this bone substitute material [8–22]. These studies showed that rates of newly built bone in the range of 23–35% were measured 6 to 7 months after its application, which is comparable to results gained by further studies by our group and others using synthetic and allografts or xenografts [8, 9, 20, 23–28].

However, studies regarding the (inflammatory) tissue reaction to Algipore®, especially in comparison to other bone substitutes, are relevant. In further studies, a correlation between the tissue responses, i.e. recruitment of multinucleated giant cells and implant bed vascularization, was shown by our group using a specialized histomorphometrical system [23–25, 29–32]. These studies revealed that the number of material-induced multinucleated giant cells, which have been shown to be involved in the degradation of other calcium phosphate-based bone substitutes, in many cases correlated with the degree of implant bed vascularization for different biomaterials or bone substitutes [23–25, 29–32]. Furthermore, it was shown that only low amounts of this multinucleated cell type were detectable in the implant beds of a xenogeneic bone substitute, whose low degradation pattern and prolonged standing time had already been described by many authors [12, 33–35]. Thus, the analysis of the inflammatory tissue response to a biomaterial further enables perspective on its regenerative potential.

Furthermore, the addition of different cell types to biomaterials has been shown to possibly influence the tissue response to a biomaterial and the outcome of (bone) tissue regeneration [36–40]. In a study by our group, the addition of monocytes to biphasic bone substitutes was analyzed, which increased the implant bed vascularization (manuscript submitted). Additionally, concepts that involve the application of autologous fibrin scaffolds and blood cells, such as granulocytes, lymphocytes, stem cells, and platelets (platelet-rich fibrin, PRF), have been shown to be favorable for cell-based tissue engineering [41, 42].

Thus, the present study primarily aimed to analyze the influence of the addition of blood to the phycogenic bone substitute on the tissue reaction with a special focus on the (inflammatory) response of the host tissue for up to 30 d after implantation by means of special histological and histomorphometrical methods using a subcutaneous implantation model in mice. Additionally, initial Fourier-transformed infrared spectroscopy (FTIR) of the bone substitute was conducted to analyze its chemical composition.

2. Materials and methods

2.1. Algipore®

Algipore® (AP, DENTSPLY Implants Manufacturing GmbH, Mannheim, Germany) is a porous natural apatite derived from red algae. It is prepared by the hydrothermal conversion of the original calcium carbonate of the algae in the presence of ammonium phosphate at approximately 700 °C, resulting in a mainly hydroxyapatite-based material, which becomes finally sterilized by gamma irradiation. It is available as granules with particle sizes of 0.3–2.0 mm and pores in the range of 5–10 μm.

2.2. FTIR spectroscopy

Recording of the IR spectra of solid samples was done using the KBr disc method. The IR spectra were recorded by an FTIR spectrometer BOMEM MB-100 (Hartmann & Braun, Canada) equipped with a standard DTGS/KBr detector, within the wavenumbers 400–4000 cm^{-1} and at resolution of 2 cm^{-1}. The spectral analyses of the FTIR spectroscopic measurements were performed with Win-Bomem Easy 3.04 software (Galactic Industries Corporation).

2.3. Animals

The study was performed on Balb/c mice that were obtained from the Military Medical Academy (Belgrade, Serbia) and with the approval of the Local Ethical Committee (Faculty of Medicine, University of Niš, Serbia). The animals were maintained for 1 week before use at the Faculty of Medicine, University of Niš, Serbia. In this experiment we used 28 males weighing between 22 and 24 g at 10 to 12 weeks of age. Animals were kept under standard conditions with regular mouse pellets, access to water ad libitum, and an artificial light–dark cycle of 12 h each.

2.4. Experimental design and subcutaneous implantation

The mice were randomly distributed into three groups. The first group ($n = 5$ animals/time point, ten animals in total) was implanted with Algipore® (AP) mixed with saline solution (group AS), and the second group ($n = 5$ animals/time point, ten animals in total) was implanted with AP mixed with blood (diluted with saline solution in the ratio 1 : 4) (group AB). Animals in the third group underwent only the surgical implantation procedure *per se* without insertion of a bone substitute (control group); four animals were included per time point (eight animals in total).

Prior to the implantation the bone substitute granules were mixed with saline solution or blood in the ratio of 1 : 1.5 per implant (10 mg of Algipore® plus 15 μl of saline solution or blood) in a sterile tissue culture plate. Blood used for implant composition was collected from the retro-orbital plexus of anesthetized Balb/c mice. Materials in both groups were implanted in the interscapular subcutaneous pockets of mice

through a minor incision using a biopsy needle. Prior to the surgical procedure, animals were anesthetized by using ketamine administered intraperitoneally.

2.5. Explantation procedure and histology

At the defined study time points (10 and 30 d after implantation), the mice were euthanized using an overdose of the aforementioned anesthetics. Immediately after euthanasia, the implanted bone substitutes were cut out together with the peri-implant tissue with a scalpel. Immediately afterward, these explants were fixed in 10% neutral-buffered formalin for 48 h and decalcified in 10% ethylenediaminetetraacetic acid (Fluka, Germany) at room temperature for 7–10 d; the further histological workup was performed at the FORM-Lab of the Clinic of Oro-Maxillofacial and Plastic Surgery of the Goethe University Frankfurt. Subsequent dehydration was achieved in a series of increasing alcohol concentrations followed by xylol. All explants were subsequently embedded in paraffin and sections with a thickness of 3–5 μm were cut using a microtome (Leica RM2255, Wetzlar, Germany). The slides were stained using the following histochemical staining: hematoxylin and eosin (HE), Azan, Trichrome Masson, and Toluidine Blue, as previously described [29]. Histochemical staining for TRAP detection was conducted to identify material-associated multinucleated giant cells and their TRAP-positive subforms as previously published [31]. Four further slides were made from each explant to conduct the immunohistochemical staining (including control slides without the primary antibody) described below.

2.6. Immunohistochemistry

Immunohistochemical detection of vessels was assessed using a mouse-specific CD31 antibody, and for the detection of murine macrophages, a mouse-specific F4/80 antibody was used as previously described [23]. Therefore, the slides were deparaffinized in four portions of xylene and hydrated in two portions of a decreasing series of ethanol followed by two portions of demineralized water. Heat-induced epitope retrieval for 30 min followed the processing steps described above. For blocking of endogenous peroxidase, a solution of 3% H_2O_2 in demineralized water was applied for 30 min. Subsequently, staining was performed with primary antibodies against the CD31 (DAKO, M0823, clone C70A) with a dilution of 1 : 50 and against a mouse macrophage-specific antibody (F4/80, eBioscience, San Diego, USA) with a dilution of 1 : 100 for 30 min in a humid chamber. The antibodies were then detected using the Dako REAL^{TM} EnVision^{TM} detection system including Peroxidase/3, 3′-Diaminobenzidine (Rabbit/Mouse-Kit, Dako, Glostrup, Denmark) that allowed visualization by DAB. Counterstaining with Mayer's hematoxylin was then applied. After dehydration by increasing ethanol concentrations up to 100% and a final treatment with xylene, the slides were coated with mounting medium and covered with coverslips.

2.7. Histological analysis

The histological analysis was performed using a Nikon light microscope (Nikon ECLIPSE 80i microscope, Tokyo, Japan) at the FORM-Lab (Frankfurt Orofacial Regenerative Medicine Laboratory of the Department for Oral, Cranio-Maxillofacial and Facial Plastic Surgery, Medical Center of the Goethe University Frankfurt). The focus of the analysis was on the evaluation of the tissue reaction and the biomaterial-specific inflammatory response to the investigated bone substitute material using an established protocol [23–25, 29–32, 35–39, 43–46]. The qualitative histological evaluation included the observation of the cells participating in the process of biomaterial integration and degradation, the implantation bed vascularization, and the possible adverse reactions such as fibrotic encapsulation or necrosis. Histological figures were captured with a microscope camera (Nikon DS-Fi1, Tokyo, Japan) that was connected to an acquisition unit (Nikon digital sight control unit, Tokyo, Japan).

2.8. Histomorphometrical measurements

The histomorphometrical analyses were conducted using an established protocol that allows the comparison of tissue reactions to different biomaterials and bone substitutes [23–25, 29–32, 35–39, 43–46]. Images of the implantation areas, i.e. so-called total scans, were obtained for the histomorphometrical analysis using a light microscope (Nikon Eclipse 80i®, Tokyo, Japan) equipped with an automatic scanning table (Prior, USA), a Nikon DS-Fi1 digital camera, and a Nikon Digital sight DS-L2 unit at ×100 magnification. The histomorphometrical analysis was performed using NIS-Elements software version 4.0 (Nikon, Tokyo, Japan). Using the Annotations and Measurements tool in the NIS Elements software, the total area of the implants, the number and the respective areas of the vessels, the numbers of multinucleated giant cells (including the TRAP-positive and TRAP-negative multinucleated giant cells), and the numbers of TRAP-positive mononuclear cells were measured on four slides from different animals per group. Vessel density on each slide was calculated as the number of vessels with respect to the total area of the explants (vessels mm^{-2}). Percent of vascularization was calculated as total vessel area/total area of explant. The numbers of TRAP-positive and TRAP-negative multinucleated giant cells and the numbers of TRAP-positive mononuclear cells were also expressed in relation to the total implantation area (cells mm^{-2}). In the case of the control groups, vascularization was measured based on the mean area measured in the implantation groups.

2.9. Statistics

The data obtained via histomorphometry were statistically analyzed by analysis of variance (ANOVA)

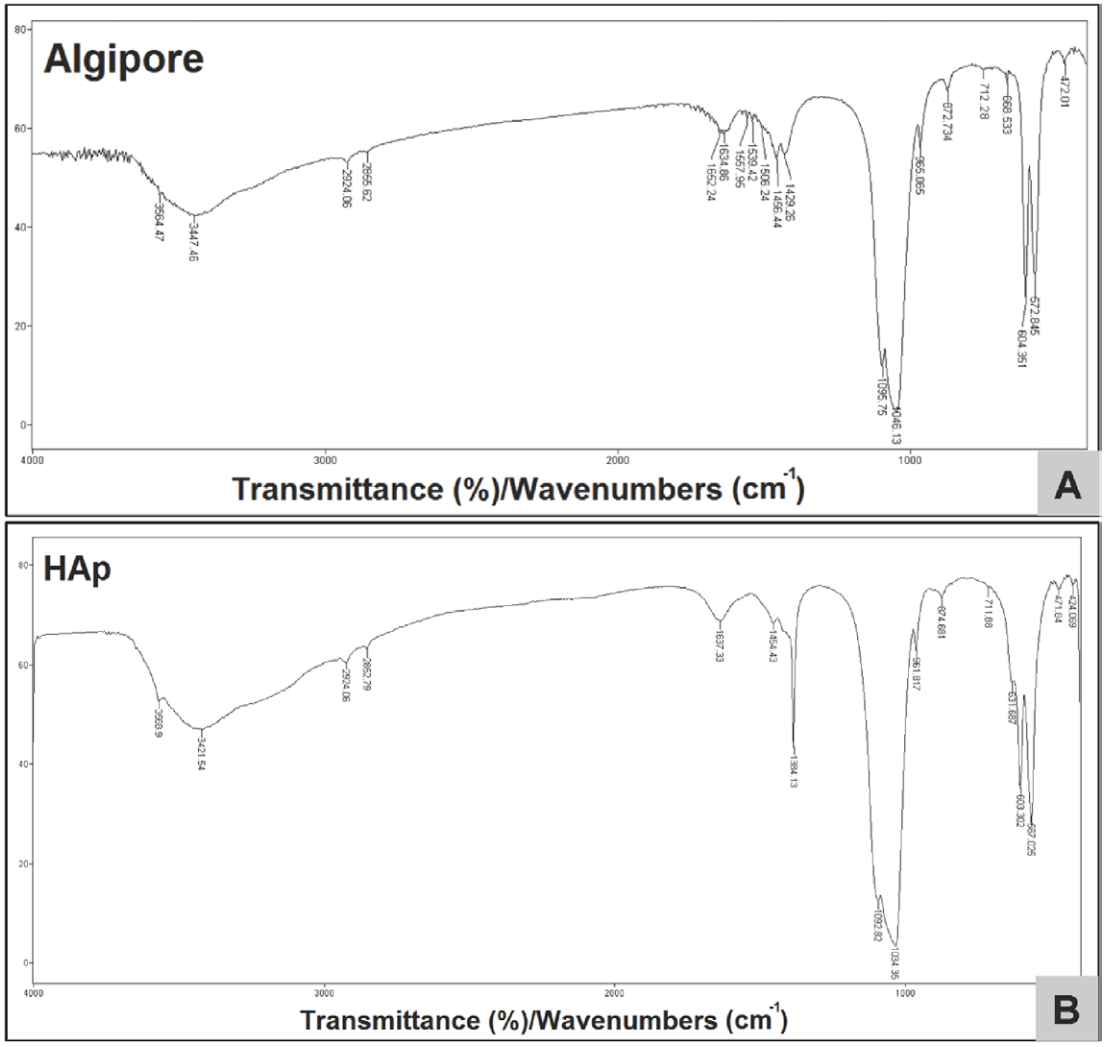

Figure 1. FTIR spectra of the Algipore® samples prior to implantation (A) and the HA test sample (B).

and following LSD post hoc assessment using SPSS 16.0.1 software (SPSS Inc., Chicago, IL). Inter- (*) and intra-individual (•) differences were regarded as significant if the respective *P*-values were less than 0.05 (*/•$P < 0.05$) or as highly significant if the *P*-values were less than 0.01 (**/••$P < 0.01$) or less than 0.001 (***/•••$P < 0.001$). Finally, the data were expressed as means and their respective standard deviations, and the GraphPad Prism 5.0 software (GraphPad Software Inc., La Jolla, CA, USA) was applied for the generation of the graphs.

3. Results

3.1. Results of the FTIR spectroscopy analysis of the blank material

The results showed that the IR spectrum of Algipore® prior to implantation was characterized by absorption bands that arise from hydroxyapatite (HAp) (figure 1(A)), determined by comparison with the IR spectrum of pure HAp standard sample (figure 1(B)). The characteristic absorption bands for HAp arise from the characteristic phosphate groups (560–640, 963 and 1028 to 1110 cm^{-1}), which can be seen as well as absorption bands that are attributed to the bending vibrations of the OH group (3572 cm^{-1}) (figure 1) [7, 8]. The characteristic absorption bands that are attributed to the stretching and bending vibrations of the C–H group can be seen and the carbonate band appears from carbonate substitution (875 and 712 cm^{-1}) for hydroxyl and phosphate groups in HAp (figure 1(A)) [47, 48].

3.2. Results of the histological analysis

3.2.1. Tissue reactions in the Algipore® plus saline (AS) group

The histological analysis revealed that the granules of the bone substitute Algipore® combined with saline (group AS) were embedded within cell-rich connective tissue at day 10 after implantation (figure 2(A)). The surfaces of the bigger material granules were mainly covered by mononuclear cells, whereas only low amounts of multinucleated giant cells were found to be related to the granule surfaces (figures 2(A) and (B)). Furthermore, the canals of the bigger bone substitute granules contained mostly low amounts of mononuclear cells at this time point (figure 2(A)). At the material surfaces of smaller material granules,

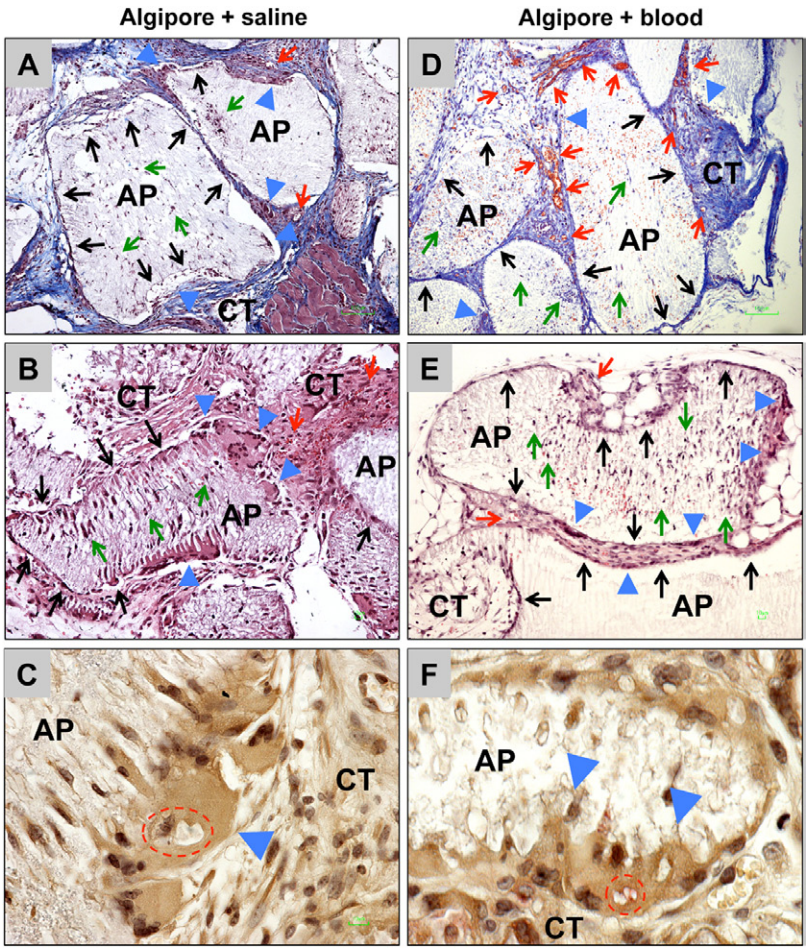

Figure 2. Tissue reactions to the Algipore® with saline (AS group) (A)–(C) and to the Algipore® with blood (AB group) (D)–(F) at day 10 after implantation. (A) and (D) The Algipore® granules (AP) in both study groups were embedded within a cell-rich and vessel-rich connective tissue (CT) at this time point. At this time point, in both groups high numbers of mononuclear cells (black arrows) were mainly found at the surfaces of the materials granules (AP), in addition to some multinucleated giant cells (blue arrow heads). Furthermore, single mononuclear cells (green arrows) were detectable within the canals of the material granules at this time point. Within the implantation beds of the AB group, higher numbers of vessels (D) were found compared to that of the AS group (A). (Azan staining, 100 × magnifications, scale bars = 100 μm). (B) and (E) At the surfaces of bigger Algipore® granules (AP), in both groups mononuclear cells (black arrows) were most often detectable, whereas only very low multinucleated giant cells (blue arrow heads) were detectable at the interface of these granules. Only a few mononuclear cells (green arrows) were observed within the canals of the bigger granules at this time point (CT = connective tissue) (HE staining, 200 × magnification, scale bars = 10 μm). (C) and (F) In both study groups the material-adherent multinucleated giant cells (blue arrow heads) have incorporated fragments (red dashed line) of the phycogenic bone substitute (TRAP staining, 600 × magnifications, scale bars = 10 μm).

relatively high amounts of multinucleated giant cells were found, and the surfaces of these granules were also covered by high amounts of mononuclear cells (figure 2(B)). The canals of the smaller material granules mostly contained higher amounts of mononuclear cells (figure 2(B)). Additionally, granulocytes, lymphocytes, and fibroblasts were found within the surrounding tissue at this time point. Additionally, the immunohistochemical detection showed that the majority of the cells within the implantation beds of the Algipore® granules and also the cells within the granules were identifiable as macrophages (figure 3(A)). Also, the multinucleated giant cells adherent to the material granules expressed the macrophage-specific antigen and contained material fragments within their cytoplasm, referring to their role in its degradation (figures 2(A) and 3(A)).

At day 30 after implantation, the above-described connective tissue was still detectable within the implantation beds of the Algipore® granules, which contained high amounts of cells (figure 4(A)). However, the connective tissue seemed to be denser at this time point in comparison to the condition at day 10 after implantation. At the surfaces of the granules, high amounts of mononuclear cells were detectable, and higher amounts of multinucleated giant cells compared with day 10 were found at this time point (figures 4(A) and (B)). Within the canals of the Algipore® granules, high amounts of mononuclear cells and micro-vessels were found (figure 4(B)). Also, at this time point, the immunohistochemical analysis showed that most of the cells at the surfaces of the granules and within the canals were macrophages (figure 3(B)). Additionally, the multinucleated giant cells at the granule surfaces

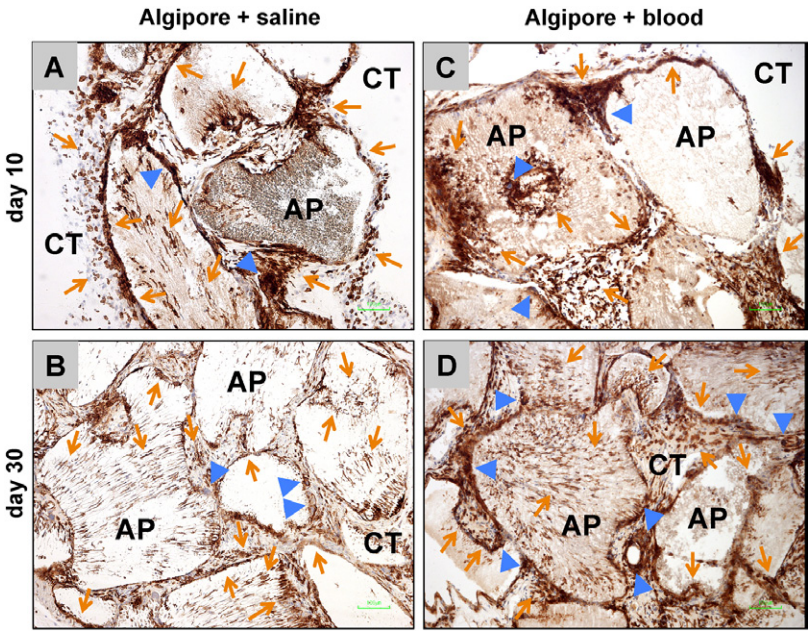

Figure 3. Representative images of the macrophage detection within the implant beds of the Algipore® with saline (AS group) (A) and (B) and the Algipore® with blood (AB group) (C) and (D). The immunohistochemical detection of the F4/80 antigen showed that most mononuclear cells within the implantation bed of the Algipore® granules (AP) and within the material canals were macrophages (orange arrows) at day 10 and day 30 after implantation. Furthermore, the staining revealed that the material-adherent multinucleated giant cells (blue arrow heads) also expressed the macrophage-specific cell surface glycoprotein (CT = connective tissue) (F4/80 immunostaining, 100 × magnifications, scale bars = 100 μm).

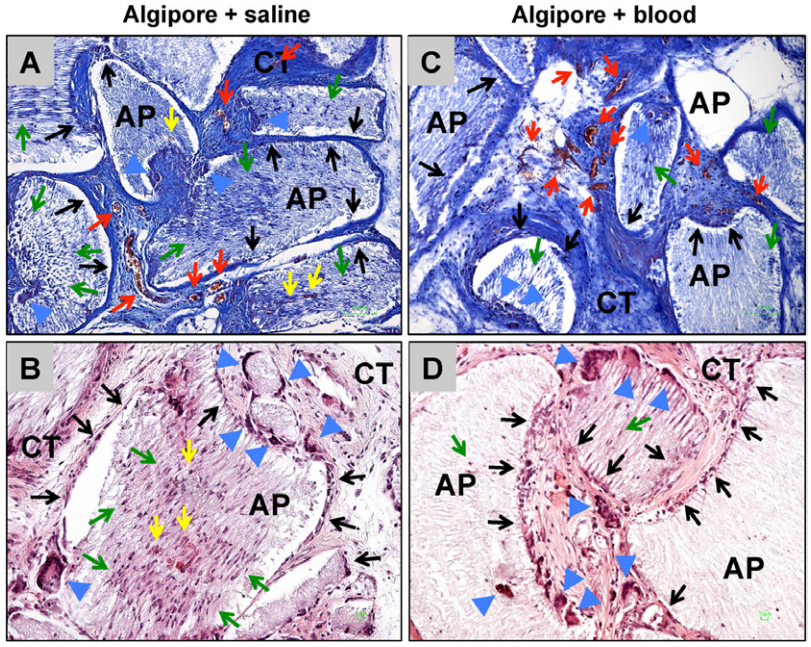

Figure 4. Tissue reactions to the Algipore® with saline (AS group) (A) and (B) and to the Algipore® with blood (AB group) (C) and (D) at day 30 after implantation. (A) and (C) In both study groups the Algipore® granules (AP) were still embedded within a vessel-rich connective tissue (red arrows = vessels). The Algipore® granules (AP) were still embedded within a cell-rich and vessel-rich (red arrows) connective tissue (CT) at this time point. At the granule surfaces, mainly mononuclear cells (black arrows) and a few multinucleated giant cells (blue arrow heads) were still found (Azan staining, 100 × magnifications, scale bars = 100 μm). (B) and (D) The multinucleated giant cells (blue arrow heads) were still mainly detectable at the surfaces of small Algipore® granules (AP), while at the surfaces of the bigger granules more mononuclear cells (black arrows) were found. At this time point, micro-vessels (yellow arrows) were found within the canals of the granules with high amounts of mononuclear cells (green arrows) (HE staining, 100 × magnifications, scale bars = 100 μm).

expressed the F4/80-antigen as shown at day 10 after implantation (figure 3(B)).

Additionally, the analysis of the vascularization revealed that moderate amounts of mainly small blood vessels were detectable within the connective tissue that surrounded the Algipore® granules (figure 5(A)). At day 30 after implantation, higher amounts of vessels with higher lumen sizes were found in the peri-implant

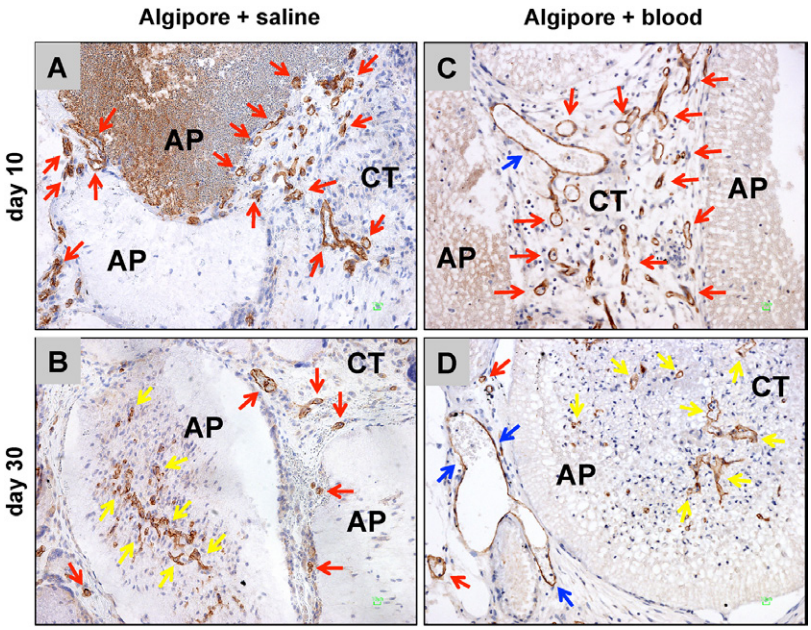

Figure 5. The vascularization pattern of the implantation beds of both study groups, i.e. the Algipore® granules (AP) without (AS group, (A) and (C)) and with the blood addition (AB group, (B) and (D)). At day 10, high numbers of microvessels (red arrows) were found within the intergranular connective tissue (CT) in the case of the AS group (A) and, in addition to microvessels, bigger vessels (blue arrows) were detected in the AB group (B). In both groups, no vessels were found within the material canals at this time point. At day 30, mainly microvessels and middle-sized vessels (red arrows) were found within the intergranular tissue of the Algipore® granules (AP) in the AS group (C), whereas mainly middle-sized and bigger vessels (blue arrows) were observable in the AB group (D). At this time point, high numbers of micro-vessels were also found within the canals of the material granules (yellow arrows) (CD31 immunostaining, 400 × magnification, scale bars = 10 μm).

tissue (figure 5(B)). Additionally, high amounts of microvessels were detectable within the canals of the Algipore® granules at this time point (figure 5(B)).

The analysis of the TRAP expression showed that only low amounts of both TRAP-positive mononucleated and multinucleated cells within the implant beds of the Algipore® granules were found at day 10 after implantation (figure 6(A)). Thus, most of the mononuclear and multinuclear cells involved in the tissue reaction to the phycogenic bone substitute material did not show signs of TRAP expression at this time point (figure 6(A)). At day 30 after implantation, higher amounts of mononucleated and multinucleated cells were TRAP-positive (figure 6(B)).

3.2.2. Tissue reactions in the Algipore® plus blood (AB) group

The histological analysis showed that the Algipore® granules were embedded within cell-rich and vessel-rich connective tissue at day 10 after implantation (figure 2(D)) Mainly mononuclear cells and some single multinucleated giant cells were present (figures 2(D) and (E)). Interestingly, the smaller material granules induced more multinucleated giant cells at their surfaces in comparison to the bigger Algipore® granules (figure 2(E)). The canals of the granules were also invaded by mononuclear cells at this time point, which mainly were detectable within the smaller granules than in the canals of the bigger Algipore® granules (figures 2(D) and (E)). The analyses furthermore showed that the multinucleated giant cells seemed to have phagocytized material fragments that were detectable within their cytoplasm (figure 2(F)).

Additionally, lymphocytes, granulocytes, and fibroblasts were detected within the peri-implant tissue.

The immunohistochemical analysis revealed that most of the mononuclear cells found in the implant beds and within the granules of Algipore® could be assigned to the macrophage line (figure 3(C)). Additionally, in this study group, the multinucleated giant cells expressed the macrophage-specific F4/80-antigen (figure 3(C)).

At day 30 after implantation, the above-described connective tissue was still found related to the Algipore® granules (figure 4(C)). Visibly higher amounts of multinucleated giant cells were found at the materials surfaces (figures 4(C) and (D)). High amounts of mononuclear cells were detectable at the granule surfaces and within the canals of the Algipore® granules, which were identified as macrophages and fused multinucleated cells that seemed to have originated from the mononuclear precursors (figures 3(D) and 4(D)).

The histological analysis of the implant bed vascularization showed that high amounts of small and large vessels were found within the connective tissue surrounding the Algipore® granules at day 10 after implantation (figure 5(C)). At day 30 after implantation, this degree of vascularization did not seem to have changed because small and large blood vessels were also found within the implantation beds of the phycogenic

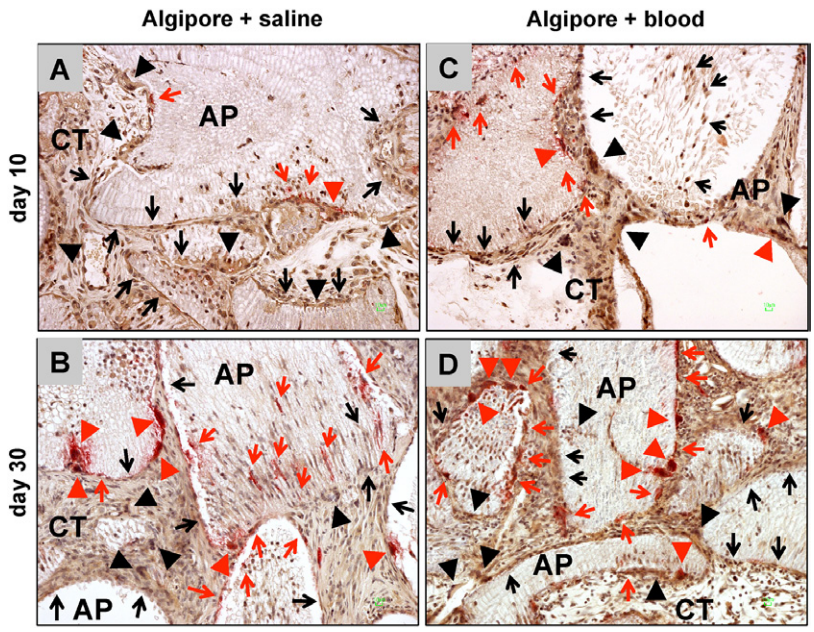

Figure 6. Representative pictures of the TRAP expression of the different cells involved in the tissue reactions to both study groups, i.e. the Algipore® granules (AP) without (AS group, (A) and (C)) and with blood addition (AB group, (B) and (D)). At day 10, most of the mononuclear cells at the surfaces of the Algipore® granules (AP) were TRAP-negative (black arrows) in both groups and only low numbers of these cells showed signs of TRAP expression (red arrows). Most of the multinucleated giant cells adhered to the granule surfaces were also TRAP-negative (black arrow heads) and only a minority of the cells of this type were TRAP-positive (red arrow heads). At day 30, higher amounts of TRAP-positive mononuclear cells (red arrows) were found within the intergranular connective (CT) and within the material canals of both study groups, whereas most of the mononuclear cells were TRAP-negative (black arrows) in both groups. At this time point, higher numbers of TRAP-positive multinucleated giant cells (red arrow heads) were found in the AB group (D) in contrast to the numbers in the AS group (C) (TRAP-negative multinucleated giant cells = black arrow heads) (TRAP staining, 400 × magnifications, scale bars = 10 μm).

bone substitute (figure 5(D)). Additionally, small vessels were found within the canals of the granules at this study time point (figure 5(D)).

Furthermore, the analysis of the TRAP expression revealed that only low amounts of the multinucleated giant cells were TRAP-positive at day 10 after implantation, whereas most of these cells did not show signs of TRAP expression (figure 6(C)). Also, low numbers of TRAP-positive mononuclear cells were detectable within the implant beds of the Algipore® granules (figure 6(C)). At day 30 after implantation, the majority of the multinucleated giant cells were TRAP-negative, and approximately one-third of these cells within the peri-implant tissue of the Algipore® granules were TRAP-positive (figure 6(D)). The analysis furthermore showed that high amounts of TRAP-positive giant cells were also found within the peri-implant connective tissue as well as at the material surfaces and within the canals of the Algipore® granules (figure 6(D)). However, most of the mononuclear cells within the implant beds were TRAP-negative (figure 6(D)).

3.2.3. Tissue reactions in the control group (sham operation)

At day 10 after implantation, the tissue around the control incisions, i.e. the mean implantation bed of the implant group, contained large numbers of mononuclear cells, including macrophages, lymphocytes, granulocytes, and fibroblasts as well as numerous vessels (figures 7(A) and (B)). The number of cells within this area was visibly larger than in unaffected areas of the subcutaneous connective tissue. At day 30 after implantation, the number of the above-described cells had decreased and wound healing was almost completed (figures 7(C) and (D)). Only some minor cell-rich foci within the subcutaneous connective tissue pointed to the former incisions, which contained mainly fibroblasts and also macrophages and single lymphocytes (figures 7(C) and (D)).

3.3. Results of the histomorphometric analyses

3.3.1. Analysis of the implant bed vascularization

At day 10 after implantation, the histomorphometrical measurements showed that both the number of vessels and the percent vessel area were significantly lower in the Algipore® plus saline (AS) group (3.22 ± 2.22 vessels mm^{-2} and 0.29 ± 0.18%) compared with the values of the Algipore® plus blood (AB) group (17.70 ± 6.18 vessels mm^{-2} and 1.01 ± 0.58%) (***$P < 0.001$) (figures 8(A) and (B)). Furthermore, the analysis showed that both parameters of the AS group were on a comparable level with that of the control group (3.73 ± 0.89 vessels mm^{-2} and 0.08 ± 0.02%). The values of the AB group were also significantly higher (***$P < 0.001$ and *$P < 0.05$) compared with those of the control group (figures 8(A) and (B)).

At 30 d after implantation, the histomorphometrical analysis showed that only an intra-individual increase of the vessel density was observed in the AS group (12.33 ± 2.80 vessels mm^{-2}), whereas

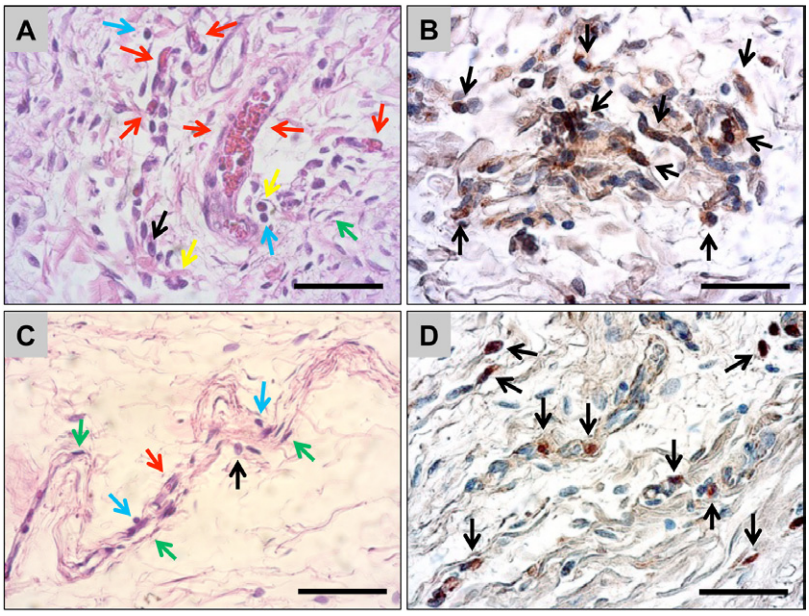

Figure 7. Representative images of the tissue reaction to the sham operations in the control group at day 10 (A) and (B) and day 30 (C) and (D). (A) At day 10, the area of the sham operation contained high numbers of different cells such as macrophages (black arrows), fibroblasts (green arrow), granulocytes (yellow arrows), and lymphocytes (blue arrows). Also, a higher vascularization (vessels = red arrows) were found in this area (HE staining, 400 × magnification, scale bar = 100 μm). (B) The immunohistochemical detection showed that most of the cells found in this area were macrophages (F4/80-immunostaining, 400 × magnification, scale bar = 100 μm). (C) At day 30 after the sham operation, only minor island-like strands in the subcutaneous connective tissue were found that contained higher amounts of the different cell types also found at day 10, i.e. mainly macrophages (black arrow), fibroblasts (green arrows), and lymphocytes (blue arrows) (HE staining, 400 × magnification, scale bar = 100 μm). (B) The immunodetection showed that at this time point macrophages (black arrows) were found randomly distributed in the former defect area (F4/80-immunostaining, 400 × magnification, scale bar = 100 μm).

this value was on a comparable level in the AB group (23.59 ± 3.89 vessels mm^{-2}), just as that of the control group (3.02 ± 0.29 vessels mm^{-2}) at this time point (figure 8(A)). The values of the AB group were significantly higher compared with those of the other groups (**$P < 0.01$ and ***$P < 0.001$) (figure 8(A)). Regarding percent vascularization, the values of all three study groups were at comparable levels as on day 10 after implantation (figure 8(B)). However, the value of the AB group (1.68 ± 0.29%) was significantly higher compared with those of the AS group (0.93 ± 0.13%) and of the control group (0.29 ± 0.06%) (*$P < 0.05$ and ***$P < 0.001$), whereas no significant differences were found between the values of the latter two groups (figure 8(B)).

3.3.2. Analysis of the multinucleated giant cells and their TRAP expression

The histomorphometrical analysis of the total amounts of multinucleated giant cells (MNGCs) showed that comparable values were found in the Algipore® + saline (AS) group (6.02 ± 1.50 MNGCs mm^{-2}) and in the Algipore® plus blood (AB) group (8.85 ± 5.09 MNGCs mm^{-2}) at day 10 after implantation (figure 8(C)). At day 30 after implantation, no changes in the amounts of the MNGCs were found in either study group, and the value in the AB group (14.33 ± 7.57 MNGCs mm^{-2}) showed a low, non-significant increase compared with the value of the AS group (8.44 ± 3.09 MNGCs mm^{-2}) (figure 8(C)).

The analysis showed that the amounts of TRAP-positive MNGCs were low in both the AS group (0.51 ± 0.45 TRAP-positive MNGCs mm^{-2}) and the AB group (0.45 ± 0.63 TRAP-positive MNGCs mm^{-2}) at day 10 after implantation without a significant difference (figure 8(D)). At day 30 after implantation, the amounts of TRAP-positive MNGCs have significantly increased in both study groups (•$P < 0.05$ and •••$P < 0.001$) (figure 8(D)). Therefore, the higher increase in the AB group (3.46 ± 1.17 TRAP-positive MNGCs mm^{-2}) was also significantly higher compared with the values in the AS group (2.38 ± 1.67 TRAP-positive MNGCs mm^{-2}) (*$P < 0.05$) (figure 8(D)).

The histomorphometrical analysis of the occurrence of TRAP-negative MNGCs showed the same tendencies as observed for the total amounts (figure 8(E)). The amounts of TRAP-negative giant cells in the AS group (6.00 ± 1.51 TRAP-negative MNGCs mm^{-2}) were slightly lower compared with the values in the AB group (8.78 ± 5.11 TRAP-negative MNGCs mm^{-2}) at day 10 after implantation (figure 8(E)). Also, at day 30 after implantation the numbers of TRAP-negative MNGCs in the AS group (6.55 ± 2.79 TRAP-negative MNGCs mm^{-2}) were lower compared with those in the AB group (10.38 ± 7.04 TRAP-negative MNGCs mm^{-2}) but without significant differences (figure 8(E)).

No (TRAP-positive) multinucleated giant cells were found in the control groups at any of the analyzed time points.

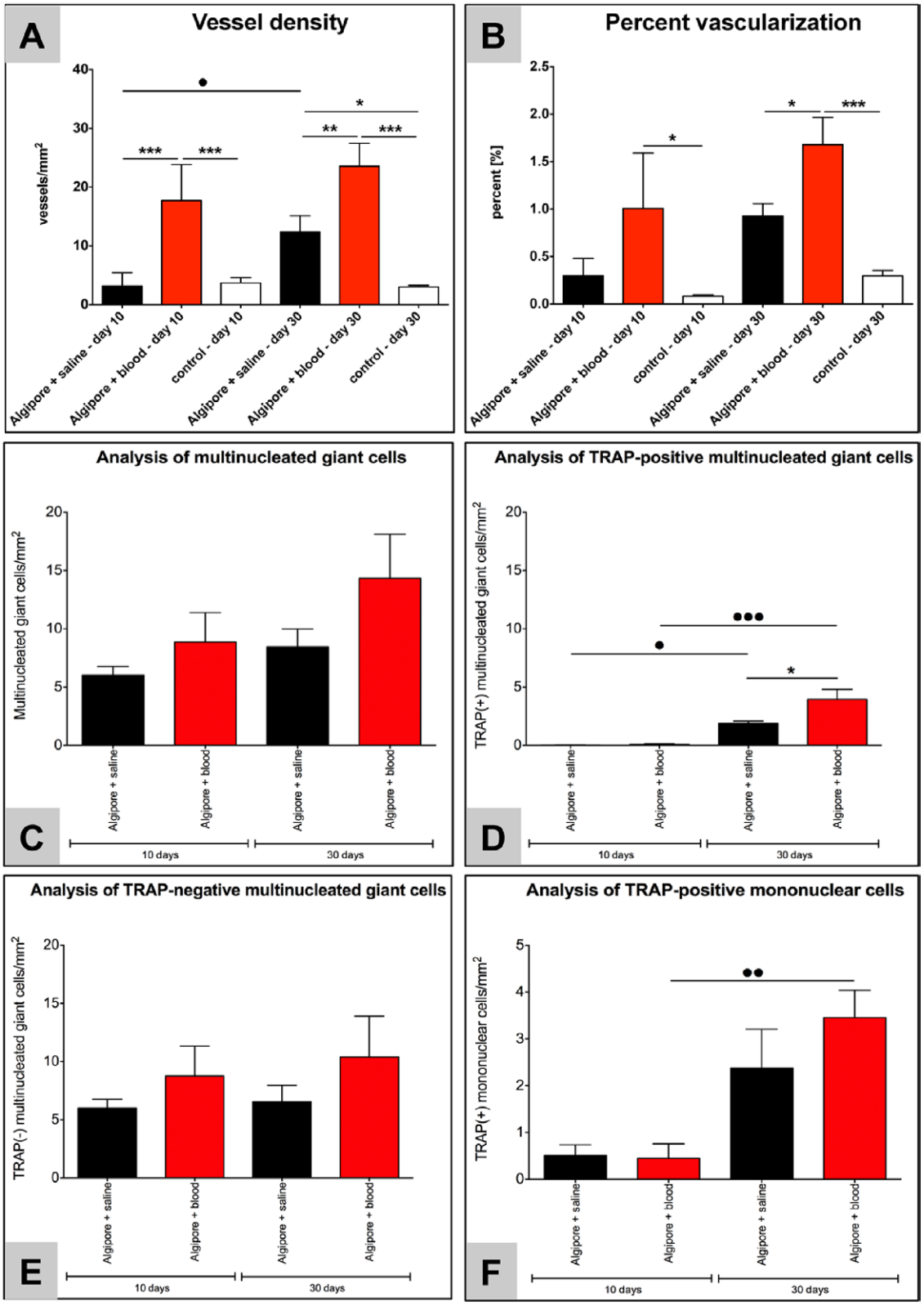

Figure 8. The results of the histomorphometrical measurements: (A) vessel density; (B) percent vascularization; (C) total numbers of multinucleated giant cells; (D) numbers of TRAP-positive multinucleated giant cells; (E) numbers of TRAP-negative multinucleated giant cells; (F) numbers of TRAP-positive mononuclear cells (*/**/*** = inter-individual statistical significances; •/••/••• = intra-individual statistical significances).

3.3.3. Analysis of the mononuclear cells and their TRAP expression

The histomorphometrical analysis showed that no differences in the TRAP expression of mononuclear cells between the AS group (0.51 ± 0.45 TRAP-positive cells mm^{-2}) and the AB group (0.45 ± 0.63 TRAP-positive cells mm^{-2}) were found at day 10 after implantation (figure 8(F)). Also, at day 30 after implantation no differences between both groups were found (AS group: 2.38 ± 1.67 TRAP-positive cells mm^{-2}; AB group:

3.46 ± 1.17 TRAP-positive cells mm^{-2}) (figure 8(F)). Although an increase of the numbers of TRAP-positive mononuclear cells was found in both groups, only a significant difference was found compared to day 10 after implantation in the AB group (●●$P < 0.01$) (figure 8(F)). No TRAP-positive mononuclear cells were found in the control groups at the both analyzed time points (data not shown).

4. Discussion

The present study aimed to analyze the effects of the addition of blood to the bone substitute material Algipore® (also commercially available as AlgOss® in Russia or as C GRAFT® in the United States), which has been shown to lead to clinically satisfying results, on the (inflammatory) tissue reactions [8, 15–22]. Its precursor material is synthesized by the marine algae *Corallina officinalis*, which is applied as a so-called phycogenic bone substitute after its thermal conversion to hydroxyapatite and its purification from organic components [15]. Interestingly, alternatives such as the phycogenic material also provide an interconnecting bone matrix-like structure as well as a natural topography [49].

Initially, it was shown via FTIR analysis that Algipore® is mainly based on hydroxyapatite, as also shown by other authors, such as for a lot of alloplastic bone substitutes [47–52]. Furthermore, the *in vivo* results revealed that the addition of blood to the bone substitute Algipore® had an impact on the tissue reaction and especially on the vascularization of the implant beds together with higher amounts of TRAP-positive multinucleated giant cells. In this context, it is known that the different blood cells can secrete different cytokines and growth factors that are involved in (bone) tissue repair and angiogenesis, such as vascular endothelial growth factor (VEGF) [53–65]. It was also shown in a further study by our group (manuscript submitted) that the addition of human peripheral blood monocytes to biphasic bone substitute materials led to an increase in vascularization. Furthermore, it was shown that the added human monocytes were involved in the tissue reactions to the bone substitute such as their murine equivalents and seemed to trigger the tissue reactions without changing its general pattern. Thus, it is presumable that the addition of the complete blood to Algipore® has also led to the inclusion of the contained cells into the tissue reactions and especially in the induction of the implant bed vascularization. Interestingly, the presented data show that only an increase of the TRAP-positive multinucleated giant cells was present after the blood addition, which might be related to the increase of the implant bed vascularization as this cell type has been shown to be a potent source of the vascular endothelial growth factor (VEGF) [30]. The increase of the TRAP-positive multinucleated cells could be related to the induction of the formation of these cell types by cytokines such as interleukin 4 (IL-4) from (added) granulocytes and lymphocytes as well as IL-13 from lymphocytes and of the granulocyte macrophage colony-stimulating factor (GM-CSF), which is secreted by lymphocytes and by macrophages themselves [66, 67]. Based on these findings, there arises the question of how these results can have an impact on the process of bone tissue regeneration. It has been revealed that inflammatory cells such as lymphocytes, granulocytes, and platelets could have an impact on bone healing by influencing the process of wound healing and additionally both the osteoblast differentiation and the velocity of the mineralization process by osteoblasts [55–61]. However, the higher vascularization should cause a higher level of regenerative bone growth, as it was shown that VEGF could induce the proliferation and differentiation of osteoblasts [2, 64, 65].

Interestingly, macrophages and lymphocytes have also been found in the control group up to day 30. In other studies the presence of inflammatory cells, i.e. mainly macrophages and cells of granulation tissue (which also includes lymphocytes), is also mentioned for the early study time points [68, 69]. Accordingly, these observed data are similar to that observed on day 15 within the present study. In contrast, at later time points no signs of inflammatory cells such as macrophages or lymphocytes are described in the literature. The condition is most often mentioned as 'normal connective tissue' or an 'absence of an inflammatory response' [70]. However, in the present study the detection of 'remnants' of the former control incisions were hardly detectable as only small cell-rich foci mainly consisting of fibroblasts and macrophages and a few lymphocytes could also be found. The detection of these small cell aggregations indicates that the process of subcutaneous wound healing has nearly reached its end. In this context it is known that these cell types are involved in the process of wound healing [55, 56, 59, 70–73]. Both macrophages and lymphocytes are involved in the collagen metabolism and modulatory processes during the healing phase [59, 71, 72]. A study by Boyce *et al* described that lymphocytes have a role in downregulating healing as a wound closes [71]. Thus, the presence of lymphocytes in all study groups including the bone substitute materials and the control group are most likely related to the healing process. However, different subtypes of lymphocytes seem to appear that can modulate both pro- and anti-inflammatory reactions [74]. This role needs to be investigated. In the context of (degradable) biomaterials, lymphocytes seem to be involved in the foreign body response by their expression of cytokines like interleukin 4 and interleukin 13 (IL-4 and IL-13), which have been revealed to be involved in the induction of the formation of BMGCs [66, 67]. Thus, the higher amounts of lymphocytes in the groups of the bone substitute material could be explained by the occurrence of both types of lymphocytes, i.e. pro- and anti-inflammatory subforms. However, no deeper understanding of the role of the single cell types and their secretion of growth factors

or cytokines exists until known, so that further studies have to be conducted to clarify their role in the process of (bone) tissue regeneration.

Additionally, the *in vivo* data of the present study show that the tissue reaction to this phycogenic bone substitute material were mainly based on mononuclear cells, i.e. macrophages. A relatively low total amount of multinucleated giant cells was detected that was comparable to values found in the implantation bed of a xenogeneic bone substitute, which was treated by high temperatures up to 1250 °C (BEGO-Oss®), and of a synthetic material based on hydroxyapatite and silica (NanoBone®) [23, 24, 29]. In contrast, Algipore® induced higher amounts of multinucleated giant cells compared with another xenogeneic bone substitute purified by temperatures of approximately 300 °C (Bio-Oss™), whose degradation was called into question because it was found in its implantation beds years after its application [33–35]. Furthermore, the numbers of multinucleated giant cells in the case of Algipore® were lower than in the case of synthetic bone substitutes on the basis of beta-tricalcium phosphate (Cerasorb® materials) [30]. This observation brings up the question of the degradation processes of this bone substitute because the induction of multinucleated giant cells and their expression of TRAP seem to be correlated with the resorption of other materials also based on hydroxyapatite and calcium phosphate [23, 24, 29–32]. Based on the present data, the resorption of this bone substitute should mainly be achieved by mononuclear cells such as macrophages, which have formerly been shown to be involved in the degradation of the aforementioned biphasic bone substitutes (manuscript submitted), although active phagocytosis by multinucleated giant cells was detected in the case of Algipore®. However, the phagocytosis capacity of mononuclear cells seems to be lower in comparison to multinuclear cells based on their lower membrane capacity. These results lead to the question of the degradability or the standing time of this bone substitute. In this context, a clinical study by Schopper *et al* described that the Algipore® granules also became degraded by multinucleated giant cells and partially replaced by newly built bone tissue 6 months after its application for sinus augmentation [8, 13]. In another study, Ewers analyzed the resorption behavior of Algipore® after its use for sinus grafting, with the result that an active resorption process was also found to be mediated by multinucleated giant cells, but only 14% volume loss was measured after 6 months [12]. The author further analyzed a biopsy sample obtained 6 years after application of Algipore®, with the results that the bone substitute was almost completely degraded and a new 'physiological' bone formation was observed [15]. Furthermore, clinical studies regarding the phycogenic bone substitute material revealed rates of newly built bone ranging from 23% to 35%, whereas the measurements showed values of remaining Algipore® between 33% and 37% and rates of connective tissue between 35% and 44% [8, 20]. In comparison to clinical results including NanoBone® and BEGO-OSS®, similar values of newly built bone were found, and lower values for the remaining bone substitutes, i.e. 24% in the case of NanoBone® and 23% in the case of BEGO-OSS®, were found [23–25]. Altogether, the described tissue response including only low amounts of multinucleated giant cells in combination with higher amounts of mononuclear cells hint at a standing time of the Algipore® material comparable to that of materials such as NanoBone® and BEGO-OSS®; this is in contrast to materials such as Bio-Oss™, which have been shown to allow rates of newly built bone between 40% and 50%, and significantly higher amounts of this material were also found [24]. Furthermore, the xenogeneic bone substitute material Bio-Oss™ was found mostly undegraded 7 years after its application for sinus augmentation [12]. Based on these findings, it is important to conduct further studies regarding the resorption pattern of that bone substitute with special focus on the degradation ability of the material-related macrophages as well as the multinucleated giant cells.

Furthermore, the results could partially elucidate the regenerative mechanisms of the phycogenic bone substitute. The granules of Algipore® are composed of naturally derived tubules that give the material a microporosity of 5–10 μm, which has been shown to allow primarily only an ingrowth of mononuclear cells, which have been shown to belong to the macrophage line by the present data. Additionally, it was revealed that many of these mononuclear cells, which had invaded the Algipore® granules in higher amounts, especially at day 30 after implantation, were TRAP-positive. Thus, it is presumable that the macrophages that invaded in the Algipore® granules were members of the pro-inflammatory M1 subpopulation because the expression of the lytic TRAP enzyme has been associated with an inflammatory differentiation state [75]. Additionally, it was shown that an ingrowth of (micro-) vessels into the Algipore® granules together with the higher invasion of (inflammatory) macrophages between day 10 and day 30 after implantation has proceeded. Thus, the induction of the intragranular vascularization seemed to be induced by the invaded macrophages, which have already been shown to be a potent source of angiogenic growth factors such as vascular endothelial growth factor (VEGF) [72].

On the basis of these results, it is further presumed that the application of Algipore® induces an ingrowth of bone tissue into the granules based on a VEGF gradient established by the invaded macrophages within the Algipore® granules. This assumption is based on study results that showed that VEGF is also able to increase the proliferation and survival of osteoblasts and could increase the level of bone formation [64]. Thus, the process of osteoconductive bone growth mediated by this bone substitute material not only should proceed on the granule surfaces but also should lead to an ingrowth of bone within its granules, which has already been described in clinical studies about Algipore® [8, 13, 15, 20].

Conclusions

The present study has initially shown that the phycogenic bone substitute material Algipore® is mostly composed of hydroxyapatite, with some carbonate content. The *in vivo* data showed that the addition of blood leads to higher implant bed vascularization, especially at day 30 after implantation, and higher numbers of TRAP-positive multinucleated giant cells. Thus, the addition of blood to a bone substitute could impact the tissue reactions, which is believed to influence the regenerative potential in bone tissue engineering/regeneration.

References

[1] Arrington E D, Smith W J, Chambers H G, Bucknell A L and Davino N A 1996 Complications of iliac crest bone graft harvesting *Clin. Orthop. Relat. Res.* 300–9

[2] Kalfas I H 2001 Principles of bone healing *Neurosurg. Focus* **10** E1

[3] Sukumar S and Drízhal I 2008 Bone grafts in periodontal therapy *Acta Med. (Hradec Kralove)* **51** 203–7

[4] Bostrom M P and Seigerman D A 2005 The clinical use of allografts, demineralized bone matrices, synthetic bone graft substitutes and osteoinductive growth factors: a survey study *HSS J.* **1** 9–18

[5] Ghanaati S, Barbeck M, Booms P, Lorenz J, Kirkpatrick C J and Sader R A 2014 Potential lack of 'standardized' processing techniques for production of allogeneic and xenogeneic bone blocks for application in humans *Acta Biomater.* **10** 3557–62

[6] Damien C J and Parsons J R 1991 Bone graft and bone graft substitutes: a review of current technology and applications *J. Appl. Biomater.* **2** 187–208

[7] Demers C, Hamdy CR, Corsi K, Chellat F, Tabrizian M and Yahia L 2002 Natural coral exoskeleton as a bone graft substitute: a review *Biomed. Mater. Eng.* **12** 15–35

[8] Schopper C, Moser D, Wanschitz F, Watzinger F, Lagogiannis G, Spassova E and Ewers R 1999 Histomorphologic findings on human bone samples six months after bone augmentation of the maxillary sinus with Algipore *J. Long Term Eff. Med. Implants* **9** 203–13

[9] Hrabák K, Szabó G, Ewers R and Gyulai-Gaál S 1999 2D and 3D computer tomography and sinus graft analysis with various graft materials *J. Long Term Eff. Med. Implants* **9** 223–33

[10] Gille J, Dorn B, Kekow J, Bruns J and Behrens P 2002 Bone substitutes as carriers for transforming growth factor-beta(1) (TGF-beta(1)) *Int. Orthop.* **26** 203–6

[11] Schlegel K A, Kloss F R, Schultze-Mosgau S, Neukam F W and Wiltfang J 2003 Osseous defect regeneration using autogenous bone alone or combined with Biogran or Algipore with and without added thrombocytes. A microradiologic evaluation *Mund Kiefer Gesichtschir.* **7** 112–8

[12] Ewers R, Goriwoda W, Schopper C, Moser D and Spassova E 2004 Histologic findings at augmented bone areas supplied with two different bone substitute materials combined with sinus floor lifting. Report of one case *Clin. Oral Implants Res.* **15** 96–100

[13] Schopper C, Moser D, Sabbas A, Lagogiannis G, Spassova E, König F, Donath K and Ewers R 2003 The fluorohydroxyapatite (FHA) FRIOS Algipore is a suitable biomaterial for the reconstruction of severely atrophic human maxillae *Clin. Oral Implants Res.* **14** 743–9

[14] Turhani D, Weissenböck M, Watzinger E, Yerit K, Cvikl B, Ewers R and Thurnher D 2005 *In vitro* study of adherent mandibular osteoblast-like cells on carrier materials *Int. J. Oral Maxillofac. Surg.* **34** 543–50

[15] Ewers R 2005 Maxilla sinus grafting with marine algae derived bone forming material: a clinical report of long-term results *J. Oral Maxillofac. Surg.* **63** 1712–23

[16] Lindenmüller I H and Lambrecht J T 2006 Sinus floor elevation and implantation--a retrospective study *Schweiz Monatsschr Zahnmed* **116** 142–9

[17] Thompson D M, Rohrer M D and Prasad H S 2006 Comparison of bone grafting materials in human extraction sockets: clinical, histologic, and histomorphometric evaluations *Implant Dent.* **15** 89–96

[18] Wanschitz F, Figl M, Wagner A and Rolf E 2006 Measurement of volume changes after sinus floor augmentation with a phycogenic hydroxyapatite *Int. J. Oral Maxillofac. Implants* **21** 433–8

[19] Kirmeier R, Payer M, Wehrschuetz M, Jakse N, Platzer S and Lorenzoni M 2008 Evaluation of 3D changes after sinus floor augmentation with different grafting materials *Clin. Oral Implants Res.* **19** 366–72

[20] Scarano A, Degidi M, Perrotti V, Piattelli A and Iezzi G 2012 Sinus augmentation with phycogene hydroxyapatite: histological and histomorphometrical results after 6 months in humans. A case series *Oral Maxillofac. Surg.* **16** 41–5

[21] Scarano A, Perrotti V, Degidi M, Piattelli A and Iezzi G 2012 Bone regeneration with algae-derived hydroxyapatite: a pilot histologic and histomorphometric study in rabbit tibia defects *Int. J. Oral Maxillofac. Implants* **27** 336–40

[22] Schulz M C, Lode A, Wittig S, Stadlinger B, Kuhlisch E, Eckelt U, Gelinsky M and Mai R 2012 Characterization of the osseointegration of Algipore and Algipore modified with mineralized collagen type I *Oral Surg. Oral Med. Oral Pathol. Oral Radiol.* **114** S160–6

[23] Barbeck M, Udeabor S, Lorenz J, Schlee M, Grosse Holthaus M, Raetscho N, Choukroun J, Sader R, Kirkpatrick C J and Ghanaati S 2014 High-temperature sintering of xenogeneic bone substitutes leads to increased multinucleated giant cell formation: *in vivo* and preliminary clinical results *J. Oral Implantol.* e-pub ahead of print

[24] Ghanaati S, Barbeck M, Lorenz J, Stuebinger S, Seitz O, Landes C, Kovács A F, Kirkpatrick C J and Sader R A 2013 Synthetic bone substitute material comparable with xenogeneic material for bone tissue regeneration in oral cancer patients: first and preliminary histological, histomorphometrical and clinical results *Ann. Maxillofac. Surg.* **3** 126–38

[25] Ghanaati S, Barbeck M, Willershausen I, Thimm B, Stuebinger S, Korzinskas T, Obreja K, Landes C, Kirkpatrick C J and Sader R A 2013 Nanocrystalline hydroxyapatite bone substitute leads to sufficient bone tissue formation already after 3 months: histological and histomorphometrical analysis 3 and 6 months following human sinus cavity augmentation *Clin. Implant Dent. Relat. Res.* **15** 883–92

[26] Ohayon L 2014 Maxillary sinus floor augmentation using biphasic calcium phosphate: a histologic and histomorphometric study *Int. J. Oral Maxillofac. Implants* **29** 1143–8

[27] Kolerman R, Samorodnitzky-Naveh GR, Barnea E and Tal H 2012 Histomorphometric analysis of newly formed bone after bilateral maxillary sinus augmentation using two different osteoconductive materials and internal collagen membrane *Int. J. Periodontics Restorative Dent.* **32** e21–8

[28] Price A M, Nunn M, Oppenheim F G and Van Dyke T E 2011 *De novo* bone formation after the sinus lift procedure *J. Periodontol.* **82** 1245–55

[29] Ghanaati S, Orth C, Barbeck M, Willershausen I, Thimm BW, Booms P, Stübinger S, Landes C, Sader R A and Kirkpatrick C J 2010 Histological and histomorphometrical analysis of a silica matrix embedded nanocrystalline hydroxyapatite bone substitute using the subcutaneous implantation model in Wistar rats *Biomed. Mater.* **5** 035005

[30] Ghanaati S *et al* 2010 Influence of β-tricalcium phosphate granule size and morphology on tissue reaction *in vivo Acta Biomater.* **6** 4476–87

[31] Ghanaati S, Barbeck M, Hilbig U, Hoffmann C, Unger R E, Sader R A, Peters F and Kirkpatrick C J 2011 An injectable bone substitute composed of beta-tricalcium phosphate granules, methylcellulose and hyaluronic acid inhibits connective tissue influx into its implantation bed *in vivo Acta Biomater.* **7** 4018–28

[32] Ghanaati S, Barbeck M, Detsch R, Deisinger U, Hilbig U, Rausch V, Sader R, Unger R E, Ziegler G and Kirkpatrick C J 2012 The chemical composition of synthetic bone substitutes influences tissue reactions *in vivo*: histological and histomorphometrical analysis of the cellular inflammatory response to hydroxyapatite, beta-tricalcium phosphate and biphasic calcium phosphate ceramics *Biomed. Mater.* **7** 015005
[33] Mordenfeld A, Hallman M, Johansson C B and Albrektsson T 2010 Histological and histomorphometrical analyses of biopsies harvested 11 years after maxillary sinus floor augmentation with deproteinized bovine and autogenous bone *Clin. Oral Implants Res.* **21** 961–70
[34] Schlegel A K and Donath K 1998 BIO-OSS—a resorbable bone substitute? *J. Long Term Eff. Med. Implants* **8** 201–9
[35] Barbeck M, Udeabor SE, Lorenz J, Kubesch A, Choukroun J, Sader R A, Kirkpatrick C J and Ghanaati S 2014 Induction of multinucleated giant cells in response to small sized bovine bone substitute (Bio-Oss™) results in an enhanced early implantation bed vascularization *Ann. Maxillofac. Surg.* **4** 150–7
[36] Fuchs S, Ghanaati S, Orth C, Barbeck M, Kolbe M, Hofmann A, Eblenkamp M, Gomes M, Reis R L and Kirkpatrick C J 2009 Contribution of outgrowth endothelial cells from human peripheral blood on *in vivo* vascularization of bone tissue engineered constructs based on starch polycaprolactone scaffolds *Biomaterials* **30** 526–34
[37] Unger R E, Ghanaati S, Orth C, Sartoris A, Barbeck M, Halstenberg S, Motta A, Migliaresi C and Kirkpatrick C J 2010 The rapid anastomosis between prevascularized networks on silk fibroin scaffolds generated *in vitro* with cocultures of human microvascular endothelial and osteoblast cells and the host vasculature *Biomaterials* **31** 6959–67
[38] Ghanaati S, Fuchs S, Webber M J, Orth C, Barbeck M, Gomes M E, Reis R L and Kirkpatrick C J 2011 Rapid vascularization of starch-poly(caprolactone) *in vivo* by outgrowth endothelial cells in co-culture with primary osteoblasts *J. Tissue Eng. Regen. Med.* **5** e136–43
[39] Ghanaati S *et al* 2011 Scaffold vascularization *in vivo* driven by primary human osteoblasts in concert with host inflammatory cells *Biomaterials* **32** 8150–60
[40] Amini A R, Laurencin C T and Nukavarapu S P 2012 Bone tissue engineering: recent advances and challenges *Crit. Rev. Biomed. Eng.* **40** 363–408
[41] Ghanaati S, Booms P, Orlowska A, Kubesch A, Lorenz J, Rutkowski J, Landes C, Sader R, Kirkpatrick C and Choukroun J 2014 Advanced platelet-rich fibrin (A-PRF)—a new concept for cell-based tissue engineering by means of inflammatory cells *J. Oral Implantol.* **40** 679–89
[42] Simonpieri A, Del Corso M, Vervelle A, Jimbo R, Inchingolo F, Sammartino G and Dohan Ehrenfest D M 2012 Current knowledge and perspectives for the use of platelet-rich plasma (PRP) and platelet-rich fibrin (PRF) in oral and maxillofacial surgery: II. Bone graft, implant and reconstructive surgery *Curr. Pharm. Biotechnol.* **13** 1231–56
[43] Ghanaati S, Orth C, Unger R E, Barbeck M, Webber M J, Motta A, Migliaresi C and James Kirkpatrick C 2010 Fine-tuning scaffolds for tissue regeneration: effects of formic acid processing on tissue reaction to silk fibroin *J. Tissue Eng. Regen. Med.* **4** 464–72
[44] Ghanaati S M, Thimm B W, Unger R E, Orth C, Kohler T, Barbeck M, Müller R and Kirkpatrick C J 2010 Collagen-embedded hydroxylapatite-beta-tricalcium phosphate-silicon dioxide bone substitute granules assist rapid vascularization and promote cell growth *Biomed. Mater.* **5** 25004
[45] Ghanaati S, Udeabor S E, Barbeck M, Willershausen I, Kuenzel O, Sader R A and Kirkpatrick C J 2013 Implantation of silicon dioxide-based nanocrystalline hydroxyapatite and pure phase beta-tricalciumphosphate bone substitute granules in caprine muscle tissue does not induce new bone formation *Head Face Med.* **9** 1
[46] Willershausen I, Barbeck M, Boehm N, Sader R, Willershausen B, Kirkpatrick C J and Ghanaati S 2014 Non-cross-linked collagen type I/III materials enhance cell proliferation: *in vitro* and *in vivo* evidence *J. Appl. Oral Sci.* **22** 29–37
[47] Ishikawa T, Wakamura M and Kondo S 1989 Surface characterization of calcium hydroxylapatite by Fourier transform infrared spectroscopy *Langmuir* **5** 140–44
[48] Reig F B, Adelantado J V and Moya Moreno M C 2002 FTIR quantitative analysis of calcium carbonate (calcite) and silica (quartz) mixtures using the constant ratio method. Application to geological samples *Talanta* **58** 811–21
[49] Tadic D and Epple M 2004 A thorough physicochemical characterisation of 14 calcium phosphate-based bone substitution materials in comparison to natural bone *Biomaterials* **25** 987–94
[50] Bohner M 2001 Physical and chemical aspects of calcium phosphates used in spinal surgery *Eur. Spine J.* **10** S114–21
[51] Eppley B L, Pietrzak W S and Blanton M W 2005 Allograft and alloplastic bone substitutes: a review of science and technology for the craniomaxillofacial surgeon *J. Craniofac. Surg.* **16** 981–9
[52] Figueiredo M, Henriques J, Martins G, Guerra F, Judas F and Figueiredo H 2010 Physicochemical characterization of biomaterials commonly used in dentistry as bone substitutes—comparison with human bone *J. Biomed. Mater. Res.* B **92** 409–19
[53] Lacy P and Stow J L 2011 Cytokine release from innate immune cells: association with diverse membrane trafficking pathways *Blood* **118** 9–18
[54] Lindemann S, Tolley N D, Dixon D A, McIntyre T M, Prescott S M, Zimmerman G A and Weyrich A S 2001 Activated platelets mediate inflammatory signaling by regulated interleukin 1beta synthesis *J. Cell. Biol.* **154** 485–90
[55] Könnecke I *et al* 2014 T and B cells participate in bone repair by infiltrating the fracture callus in a two-wave fashion *Bone* **64** 155–65
[56] Nam D, Mau E, Wang Y, Wright D, Silkstone D, Whetstone H, Whyne C and Alman B 2012 T-lymphocytes enable osteoblast maturation via IL-17F during the early phase of fracture repair *PLoS One* **7** e40044
[57] Canalis E, McCarthy T L and Centrella M 1991 Growth factors and cytokines in bone cell metabolism *Annu. Rev. Med.* **42** 17–24
[58] Kawaguchi H 2009 Bone fracture and the healing mechanisms. Fibroblast growth factor-2 and fracture healing *Clin. Calcium* **19** 653–9
[59] Andrew J G, Andrew S M, Freemont A J and Marsh D R 1994 Inflammatory cells in normal human fracture healing *Acta Orthop. Scand.* **65** 462–6
[60] Mumme M *et al* 2012 Interleukin-1β modulates endochondral ossification by human adult bone marrow stromal cells *Eur. Cell Mater.* **24** 224–36
[61] Glass G E, Chan J K, Freidin A, Feldmann M, Horwood N J and Nanchahal J 2011 TNF-alpha promotes fracture repair by augmenting the recruitment and differentiation of muscle-derived stromal cells *Proc. Natl Acad. Sci. USA* **108** 1585–90
[62] Lin Z Q, Kondo T, Ishida Y, Takayasu T and Mukaida N 2003 Essential involvement of IL-6 in the skin wound-healing process as evidenced by delayed wound healing in IL-6-deficient mice *J. Leukoc. Biol.* **73** 713–21
[63] Sander A L, Henrich D, Muth C M, Marzi I, Barker J H and Frank J M 2009 *In vivo* effect of hyperbaric oxygen on wound angiogenesis and epithelialization *Wound Repair Regen.* **17** 179–84
[64] Harper J and Klagsbrun M 1999 Cartilage to bone—angiogenesis leads the way *Nat. Med.* **5** 617–8
[65] Johnson K E and Wilgus T A 2014 Vascular endothelial growth factor and angiogenesis in the regulation of cutaneous wound repair *Adv. Wound Care (New Rochelle)* **3** 647–661
[66] Chang D T, Jones J A, Meyerson H, Colton E, Kwon I K, Matsuda T and Anderson J M 2008 Lymphocyte/macrophage interactions: biomaterial surface-dependent cytokine, chemokine, and matrix protein production *J. Biomed. Mater. Res.* A **87** 676–87
[67] Brodbeck W G, Macewan M, Colton E, Meyerson H and Anderson J M 2005 Lymphocytes and the foreign body

response: lymphocyte enhancement of macrophage adhesion and fusion *J. Biomed. Mater. Res.* A **74** 222–9
[68] Ye Q, Ohsaki K, Ii K, Li D J, Matsuoka H, Tenshin S and Yamamoto T 1998 A subcutaneous tissue reaction in the early stage to a synthetic auditory ossicle (Bioceram) in rats *J. Med. Invest.* **44** 173–7
[69] Marković D, Kojić Z, Marinković D, Danilović V, Radovanović A and Janaćković Đ 2009 Histological and immunohistochemical evaluations of rat soft tissue response to bioceramical implants *Acta Veterinaria (Beograd)* **59** 243–53
[70] da Cruz A C, Pochapski M T, Daher J B, da Silva J C, Pilatti G L and Santos F A 2006 Physico-chemical characterization and biocompatibility evaluation of hydroxyapatites *J. Oral. Sci.* **48** 219–26
[71] Boyce D E, Jones W D, Ruge F, Harding K G and Moore K 2000 The role of lymphocytes in human dermal wound healing *Br. J. Dermatol.* **143** 59–65
[72] Brancato S K and Albina J E 2011 Wound macrophages as key regulators of repair: origin, phenotype, and function *Am. J. Pathol.* **178** 19–25
[73] Bainbridge P 2013 Wound healing and the role of fibroblasts *J. Wound Care.* **22** 407–8, 410–2
[74] Abbas A K, Murphy K M and Sher A 1996 Functional diversity of helper T lymphocytes *Nature* **383** 787–93
[75] Janckila A J, Slone S P, Lear S C, Martin A and Yam L T 2007 Tartrate-resistant acid phosphatase as an immunohistochemical marker for inflammatory macrophages *Am. J. Clin. Pathol.* **127** 556–66